

Received June 11, 2021, accepted June 24, 2021, date of publication July 2, 2021, date of current version July 14, 2021.

Digital Object Identifier 10.1109/ACCESS.2021.3094279

UWB-Based Safety System for Autonomous Guided Vehicles Without Hardware on the Infrastructure

LETICIA ZAMORA-CADENAS^{1,2}, IGONE VELEZ^{1,2}, AND J. ENRIQUE SIERRA-GARCIA^{3,4}

¹ICT Division of CEIT, Basque Research and Technology Alliance (BRTA), 20018 San Sebastian, Spain

²Tecnun, Universidad de Navarra, 20018 San Sebastian, Spain

³Department of Electromechanical Engineering, University of Burgos, 09006 Burgos, Spain

⁴ASTI Mobile Robotics, 09390 Madrigalejo del Monte, Spain

Corresponding author: Leticia Zamora-Cadenas (lzamora@ceit.es)

This work was supported in part by the Ministerio de Ciencia e Innovación of the Spanish Government through the Project SAFE-AGV under Grant RTC-2017-6043-7, and in part by the Basque Government through the Project Autoev@1.

ABSTRACT Automated Guided Vehicles (AGV) are unmanned transport vehicles widely used in the industrial sector to substitute manned industrial trucks and conveyors. In order to guarantee safe operation, AGVs must be equipped with a safety system to stop their movement in presence of obstacles or humans in their path. This work presents a novel safety system for AGVs that is based on Ultra Wideband (UWB) technology. Unlike previous works based on UWB Real-Time Location Systems (RTLS), the proposed safety system does not require installing hardware on the plant's infrastructure. Instead, the AGV is equipped with sensors capable of locating the tag of a person or a mobile asset. This simplifies deployment of the solution and enables its use in dynamic environments. The proposed safety system was mounted in an AGV designed by the company ASTI Mobile Robotics. Dynamic measurements showed that the proposed safety system accurately mirrors the relative movement between the AGV and tag. Furthermore, the proposed safety system employs a novel method for post-processing ranging data. Measurements showed that this method improves the accuracy of the system, resulting in a more homogeneously distributed positioning error around a room.


INDEX TERMS Autonomous vehicle, automated guided vehicle (AGV), indoor navigation, real-time location system (RTLS), robot sensing system, ultra-wideband (UWB) technology, vehicle safety.

I. INTRODUCTION

Nowadays, many industrial processes suffer from high product variability and, at the same time, shortened product-life cycles. This requires an agile and flexible production structure that can be reconfigured rapidly to meet new product demands [1]. This degree of flexibility cannot be achieved by traditional automation. However, the emerging technologies in Industry 4.0 are the ones that will allow highly-flexible production systems. In this scenario the autonomous mobile robots will increase the flexibility and productivity of many industrial processes [2].

Automated Guided Vehicles (AGV) are unmanned transport vehicles currently used in the industrial sector to

substitute manned industrial trucks and conveyors. This kind of mobile robots usually navigates by following long marked lines or magnetic tapes on the floor. Recent advances in Artificial Intelligence have allowed these mobile robots to move in a more autonomous way, without the need for marks on the floor. These autonomous AGVs allow greater flexibility in the production structure, as they do not need to drive in a predefined area [2]. However, these autonomous AGVs share the work-space with humans, manned industrial trucks and other mobile assets. In order to guarantee their safe operation, AGVs must be equipped with a safety system to stop their movement in the presence of obstacles in the path [3]. Moreover, multi-sensor systems are used to improve the navigation of AGVs in these variable environments. Among others, encoders, gyroscopes, ultrasound sensors, infrared sensors, LIDARs (Laser Imaging Detection and Ranging),

The associate editor coordinating the review of this manuscript and approving it for publication was Thomas Canhao Xu .

RADARs (Radio Detection And Ranging) or cameras are commonly used for safe indoor navigation of AGVs [4], [5].

Ultrasound sensors and LIDARs can also be employed as a safety system to avoid collisions with AGVs: if they sense something is in the path, the AGV must stop prior to impact. Ultrasound sensors are low-cost solutions but their range and reliability is not usually sufficient for industrial applications. LIDARs provide high reliability but they are expensive [6]. Furthermore, they have several major drawbacks. They cannot cover 360° around the AGV, which forces two LIDARs to be installed per vehicle, increasing the cost of the system even more. Additionally, LIDARs only provide two-dimensional (2D) information about an obstacle at a specific height from the floor, usually a few centimeters above the floor. Thus, in many cases additional vertical safety LIDARs must be installed, making the final cost of the safety system very expensive. Finally, if these systems are used in highly changing environments or crowded areas, the AGVs are constantly stopped, and the technology becomes ineffective. The AGVs should be able to distinguish between the possible obstacles they sense in their path and react accordingly: sometimes it may be enough to simply change their route; other times they must stop, especially if they are in a person's path.

In recent years, Real-Time Location Systems (RTLSS) have been used to identify and track the location of people or objects in indoor environments in real time. These systems can also help AGVs navigate more safely in a production plant [7]. RTLSSs can be used to estimate the position of the AGV within the production plant. Additionally, they can be used to locate people wearing a tag near the AGV and thus avoid a collision between an AGV and a person. Obviously, the accuracy of the RTLSS is a key aspect when it is used as a safety system for an AGV that moves around people.

Although some RTLSSs use optical (usually infrared) or acoustic (usually ultrasound) technologies, the physical layer of RTLSS is usually based on radio-frequency (RF) communication. The accuracy of RTLSSs depends on the RF technology used. We can find RTLSSs based on WiFi, Bluetooth, Zigbee or Chirp Spread Spectrum (CSS), but Impulse Radio Ultra Wideband (IR-UWB) is considered the most promising technology for indoor positioning [8]. IR-UWB is based on the transmission of radio signals that occupy a very large bandwidth. This technology performs robustly in multipath channels. Its high accuracy in the time-of-flight estimation has made it really attractive for estimating the position of a node. A detailed comparison of different IR-UWB based positioning solutions can be found in [8] and [9].

There are various articles in the literature that use RTLSS systems to help AGVs navigate indoors. For example, in [10] and [11] CSS-based sensors were used in combination with laser range finders for mobile robot navigation. Recently, RTLSS systems based on IR-UWB have been proposed for locating AGVs indoors [6], [12]–[14] or Unmanned Aerial Vehicles (UAVs) [15]. The higher accuracy of IR-UWB technology improves the AGVs' ability to navigate. IR-UWB can also be combined with information from other sensors.

In [16] and [17], UWB technology was combined with inertial sensors to achieve greater accuracy. [18] combined UWB technology with computer vision for AGV navigation; [19] combined UWB, inertial sensors and vision for small Unmanned Aerial Vehicle (Mini-UAV) localization indoors. Recently, [20] proposed placing a bigger number of nodes in the AGV to improve the availability and accuracy of the AGV positioning estimates in the situation of signal blockage caused by obstacles and carried cargoes. Nevertheless, in all these works, some nodes (anchors) were installed on the plant infrastructure so that the RTLSS could provide the position of a target node placed in the AGV. These solutions can be expensive if a large area needs to be covered. Moreover, in the highly-flexible Industry 4.0 production scenarios, having fixed infrastructure may not be the best idea, as any change in the production system's layout can reduce the system's accuracy.

Reference [21] proposed to combine UWB, GNSS, inertial sensors and vision for outdoors positioning of intelligent vehicles. Once more, some nodes (anchors) were needed to be installed outdoors so that the UWB RTLSS could work. Placing anchors outdoors can be expensive if the vehicle needs to travel large distances. Reference [22] proposed to combine UWB and wheel-speed sensors as a collision warning system for road vehicles. However, this solution does not consider the safety of people moving around these vehicles.

Recently, [23] proposed to use UWB as a collision avoidance systems for Automated Guided Vehicles. However, it keeps requiring to install some sensors on the plant infrastructure. Reference [24] was the first to propose a collision avoidance system for Automated Guided Vehicles based on Ultra-Wideband technology and without requiring hardware to be installed on the plant infrastructure. The system estimated the distance between a node in the AGV and the target node to detect if the target node was within a certain safe distance from the AGV. Nevertheless, the system proposed in [24] was not able to determine the exact location of the target node, so the AGV could not detect if the target node was in the AGV's trajectory. Moreover, the collision avoidance system in [24] suffered from errors in estimating distance above ten meters. Such outliers must be detected and eliminated if this system is to be used as an AGV safety system.

Different methods can be found in the literature to improve the accuracy of the distance estimates and eliminate these outliers, as, in fact, the accuracy in the distance estimates significantly affects the accuracy of the positioning estimates in a RTLSS system. Reference [25] presented a method for post-processing CSS data that significantly improved the accuracy of the distance estimator. Recently, [21] proposed to use a similar method to improve the accuracy of IR-UWB based distance estimates. The work in [26] evaluated different distance error calibration methods for indoor UWB positioning applications and [27] proposed a method to post process the distance estimates while auto-positioning the anchors. However, all these methods require to perform a calibration in the same place where the RTLSS system is going to be used.

Thus, this calibration should be repeated if there are changes in the layout of the plant where the AGV is working.

This paper proposes a novel safety system based on IR-UWB that does not require hardware to be installed on the plant infrastructure. The proposed safety system is able to provide the position of the target node with high accuracy, which makes its use appealing in the highly-flexible Industry 4.0 production scenarios. In order to improve the accuracy of the positioning estimates, a simple method for post-processing ranging data is also proposed in this work, which does not require in-site calibration.

The rest of this paper is structured as follows. Section II summarizes the main characteristics of the traditional RTLS based safety systems. Section III describes the proposed UWB-based safety system. Section IV presents and discussed the experimental results obtained with the proposed system. Finally, Section V summarizes the main conclusions of this work.

II. TRADITIONAL RTLS-BASED AGV NAVIGATION SYSTEMS

As explained above, RTLSs can help AGVs navigate safely indoors. There are many works in the literature that propose using these location systems in AGV navigation [6], [7], [10]–[14], [16]–[20]. In this section, we will overview the main characteristics of the current RTLS-based safety systems for AGVs.

A. BASIC ARCHITECTURE OF A REAL-TIME LOCATION SYSTEM

A typical RF location system for indoor environments consists of a set of anchors, whose positions $(x_{an_j}, y_{an_j}, z_{an_j})$ are known, and one or more tags, whose positions (x_i, y_i, z_i) are the ones to be determined [28]–[37]. Such systems rely on a fixed infrastructure composed of anchors, and will be referred to as Fixed-Infrastructure RTLS (FI-RTLS) in this paper. Fig. 1 shows the basic architecture of an FI-RTLS for indoor environments. The image shows a system with four anchors, four tags and one Central Unit (CU). The location of each tag is estimated in two steps: ranging and positioning.

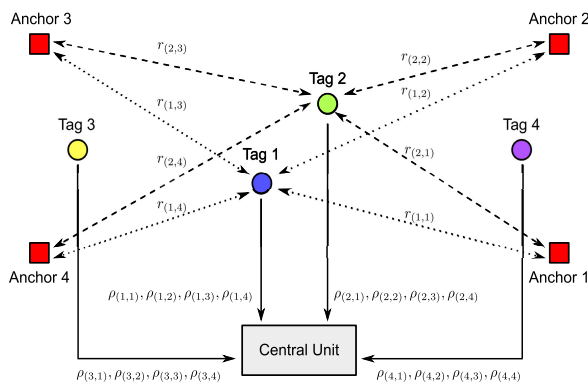


FIGURE 1. Basic architecture of an FI-RTLS for indoor environments.

Firstly, the ranging estimates (angle, received power or time of flight) between each anchor and the tags, $\hat{\rho}_{(i,j)}$, are calculated using ranging algorithms such as in [34], [38]–[43]. These ranging estimates are not usually equal to the real value $\rho_{(i,j)}$, since errors in the transmission or multipath can deteriorate the signals. Secondly, the position of each tag, (x_i, y_i, z_i) , is estimated in the CU using these ranging estimates. In Fig. 1 the transmitted signal $r_{(i,j)}$ from the j^{th} anchor to the i^{th} tag is also represented.

The type of system presented in Fig. 1 is called a tag-based system. In this kind of system, the tag collects the ranging estimates, $\hat{\rho}_{(i,j)}$, and sends them to the CU. The tag can also estimate the position with these ranging estimates, and then, can send these positioning estimates to the CU. When each anchor collects the ranging estimates and transmits them to the CU so that the position is estimated there, the system is called an anchor-based system.

One of the main challenges of indoor location with RF technology is the multipath effect. Indoor environments produce multiple replicas of the transmitted signal due to reflections caused by, for example, very close objects. Additionally, sometimes, the direct path can be shadowed and might not be the strongest path. Such a situation normally leads to severe degradation in ranging performance in narrowband location systems, and thus to degradation in location accuracy. An effective way to cope with the multipath effect is to increase the bandwidth of the signal transmitted by the tag [44]. Thus, the large bandwidth of IR-UWB makes it the best candidate for an RTLS system used indoors [8].

B. FI-RTLS AGV NAVIGATION SYSTEM

In intralogistic systems, AGVs work in a fleet. The behavior of the fleet as a whole is controlled by a Fleet Control System (FCS), which shares production information with the factory’s Enterprise Resource Planning system (ERP). Using this information, the FCS sends orders to the AGVs that include origin station, the destination station and the route to be taken. Without an RTLS system that is able to locate AGVs, other mobile robots and people, route assignment occurs without information regarding the presence of people or mobile assets being taken into account. This lack of information may lead to the FCS using congested zones, resulting in unnecessary stops and ultimately reducing the productivity of the plant. It is clear, therefore, that the positioning information provided by an RTLS system can improve the navigation of a fleet of AGVs.

Fig. 2 shows the basic architecture of an FI-RTLS AGV navigation system. Anchors are fixed on the plant’s infrastructure, usually on the walls, and AGVs and workers carry one tag each. If a tag-based FI-RTLS system is used, the positions of the tags are sent to the FCS via a wireless link. This link could be the same one used in the positioning estimation (IR-UWB) or a different one. This communication link increases the tag’s power consumption, thereby reducing its battery life. In an anchor-based FI-RTLS system, a CU

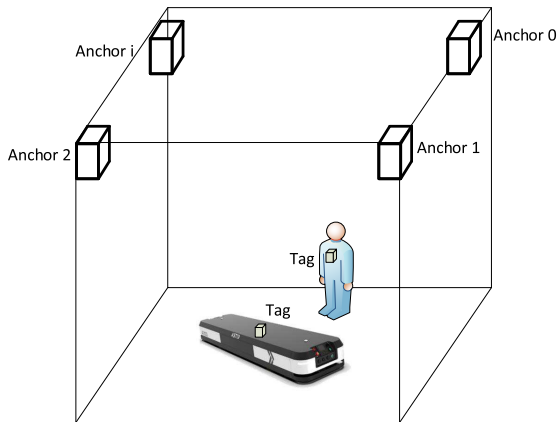


FIGURE 2. Basic architecture of an FI-RTLS AGV navigation system.

collects all the ranging data to produce a positioning estimate, which is sent to the FCS.

Both cases require an ultra-low latency communication link between FCS and the AGVs if the FCS commands are going to be used as a safety system, i.e.: to stop an AGV if it is going to collide with an obstacle. 5G technology is meant to provide the latency required by these kinds of applications, but it is not yet in widespread use. Until then, the positioning information from the FI-RTLS AGV navigation system is mainly used by the FCS to monitor the movement of the AGVs.

In any case, the biggest drawback of current FI-RTLS AGV navigation systems is that they still require anchors to be installed in different locations of the plant. The anchor placement significantly affects the accuracy of the system, so the deployment of an FI-RTLS system should be done carefully. In fact, many of the FI-RTLS systems require an on-site calibration step to achieve good accuracy [45]. However, given the high product variability and the shortened product-life cycles that characterize industry today, the production plant layouts change from time to time, which will affect the accuracy of an FI-RTLS system. Any change in the layout may involve changing the location of the anchors and/or a repetition of the calibration procedure, which can be time-consuming and expensive.

III. DESCRIPTION OF THE PROPOSED NFI-RTLS AGV SAFETY SYSTEM

A. PROPOSED ARCHITECTURE

Fig. 3 presents the architecture of the proposed UWB-based safety system for AGVs. Unlike traditional RTLS-based solutions, the safety system for AGVs proposed in this work does not require anchors be installed on the infrastructure. It only requires some sensors be installed in the AGV to locate the tag of a person or mobile asset. Thus, the proposed safety system will be based on a non-fixed infrastructure real-time location system, which we denote as NFI-RTLS AGV safety system in this work. As no fixed infrastructure is required, the proposed system does not depend on the factory layout and simplifies

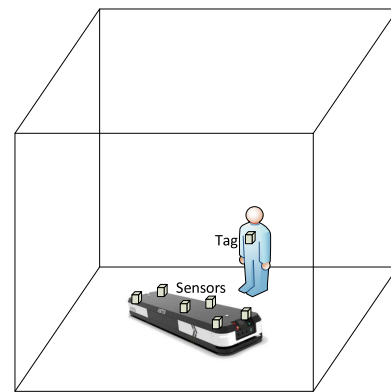


FIGURE 3. Architecture of the proposed NFI-RTLS AGV safety system.

the deployment of the safety system and thus the use of AGVs in a production plant. Moreover, the proposed system will provide the factory with the flexibility demanded by Industry 4.0 production scenarios.

Fig. 4 shows how the sensors are placed in an AGV. In the figure, four IR-UWB sensors are placed at the corners of the AGV, and two are placed at the middle of the long edges. These sensors communicate via IR-UWB with the tag worn by people in the factory or placed on other moving vehicles or assets. The Time-of-Flight of the transmitted signal is used to estimate the rangings between the tag and each of the sensors on the AGV.

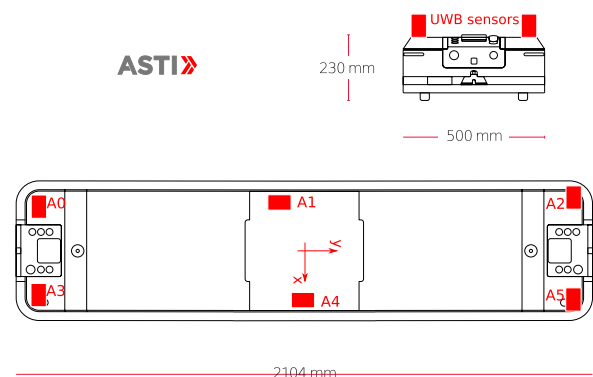


FIGURE 4. Placement of the UWB sensors in the AGV.

In Fig. 4, the antennas of the sensors are oriented facing out the AGV. Note that this means that if a tag is placed near one side of the AGV, the sensors that are in the opposite side are not in direct line-of-sight (LOS) of the tag. Thus, the NFI-RTLS-based AGV safety system will always be working with some non-line-of-sight (NLOS) ranging estimates. Additionally, the system can suffer shadowing if the tag is worn by a person. If this is the case, methods to mitigate the body shadowing such as [46] can be implemented in this system.

B. RANGING POSTPROCESSING

Due to errors in the communication between the tag and the sensors, the ranging estimator may also produce certain

inconsistent data, such as negative ranging data, that must be eliminated. Additionally, this ranging estimation presents a degree of bias and produces outliers that decrease the accuracy of the positioning algorithms. Thus, similar to [25], in this proposed NFI-RTLS AGV safety system, negative ranging data and outliers are eliminated. [25] also proposed post-processing the ranging estimates using the following equation:

$$\rho_{m,j}^{(1)} = \alpha \cdot \rho_{m,j}^{(0)} + \beta, \quad (1)$$

where α and β are empirical parameters that correct the estimated distance between tag and sensor and $\rho_{m,j}^{(0)}$ is the m^{th} ranging estimate between the tag and the j^{th} sensor after negative numbers and outliers are eliminated. $\rho_{m,j}^{(1)}$ is the m^{th} post-processed ranging estimate between the tag and the j^{th} sensor that will be used in the positioning algorithm.

In order to calculate the empirical parameters in (1), [25] proposed estimating different values of α and β for each sensor. However, in our work the same values of α and β are proposed to be used for all sensors, as it simplifies the calibration procedure and the estimated values of these parameters significantly improve the ranging accuracy of the system. Thus, in this calibration step, M measurements should be performed by placing the tag at different distances from a sensor on different days and under different conditions. Because it is not necessary to perform these measurements in the same place where the AGV will be used, these measurements can be taken during the AGV's production phase. Furthermore, there is no need to repeat this calibration procedure if there are changes in the layout of the plant where the AGV is working. Thus, the installation procedure of the sensors is simple: first, a tag and a sensor are used to estimate the α and β parameters. Then, the sensors are placed in the AGV and connected to the battery of the AGV.

Let \mathbf{d} be a vector with M real distances between the tag and the sensor and $\mathbf{d}^{(0)}$ the vector with the M distances obtained after eliminating the negative ranging data and the outliers. Then, parameters α and β are estimated by applying linear regression to:

$$\mathbf{d} = \alpha \cdot \mathbf{d}^{(0)} + \beta. \quad (2)$$

C. SAFETY SYSTEM ALGORITHM

The ranging information is post-processed according to (1) and the empirical parameters are estimated using (2). These post-processed ranging estimates are employed to calculate the relative position of the tag within the reference coordinate system of the AGV. In this work, an extended Kalman filter (EKF) was used to estimate this position of the tag [47].

The position information of the surrounding tags is provided to the AGV's CU, so that it can decide the next step in the trajectory. Furthermore, this safety system allows individual identification of the tags. In this way, it is possible to know whether the tag is attached to a person or to another mobile robot, allowing these decisions to be made more appropriately for each case. For example, if the person has experience

working with AGV, safety limits could be reduced; or if the load transported by a certain manned vehicle is dangerous, these limits could be extended. Traditional safety sensors, such as bumpers, ultrasounds or LiDARs, only detect the objects but cannot identify them.

Considering the tags detected, the AGV needs to reduce its maximum cruise velocity v_{\max} according to the following expression:

$$v_{\max} = -\tau_{\text{lat}} \cdot b_r + \sqrt{\tau_{\text{lat}}^2 \cdot b_r^2 + 2 \cdot r_{\min} \cdot b_r}, \quad (3)$$

where b_r is the braking deceleration rate of the AGV; τ_{lat} is the latency of the system and r_{\min} is the minimum distance between the AGV and the safety zone of the person or asset for a safe trajectory. This minimum distance is given by

$$\begin{aligned} r_{\min} &= \min(\sqrt{x_i^2 + y_i^2} - S_{d_i} - \tilde{\epsilon}_{r_i}) \\ &= \min(r_i - S_{d_i} - \tilde{\epsilon}_{r_i}), \end{aligned} \quad (4)$$

where (x_i, y_i) is the relative position between the AGV and the tag i and thus r_i is the radius of this position in polar coordinates, when the coordinate center is on the AGV. In addition, S_{d_i} is the safety distance associated to the asset or people monitored by tag i , and $\tilde{\epsilon}_{r_i}$ is the estimation of the radial error in the measurement of the tag i .

The deceleration rate b_r depends on the type of AGV and the type of load to be transported, since it is related to the parameters of the system dynamics, such as inertia. The AGV knows its load, thus b_r is properly updated while the system is working. The tag identification (ID) is used to classify it as representing a human or mobile asset. Different safety distances S_{d_i} could be assigned to each tag according to the object or person monitored.

The proposed NFI-RTLS AGV safety system can be used to decide when the AGV and the tag are below a reaction distance r_{d_i} :

$$r_i < r_{d_i} = v \cdot \tau_{\text{lat}} + \frac{v^2}{2 \cdot b_r} + S_{d_i} + \tilde{\epsilon}_{r_i}, \quad (5)$$

where v is the current velocity of the AGV. Thus, for each positioning estimate the CU receives, v_{\max} is computed using (3). Whenever the distance between tag and AGV is below r_{d_i} as defined in (5), the AGV should react by reducing its cruise velocity below v_{\max} . Note that this means that the AGV should start braking when the radius of polar coordinate system r_i is below the reaction distance r_{d_i} . This way, the AGV will be able to maintain a safety distance S_{d_i} from the person or asset and, thus, avoid any collision with them. Fig. 5 shows the relation between r_{d_i} and S_{d_i} .

In some situations people may not notice the AGV. To address this issue, the safety jacket which contains the UWB tag will be equipped with an electronic device to notify the operator by acoustic signals and vibration when the user has crossed a warning zone.

Moreover, the AGV's navigation system can exploit the information about the relative position of the tag provided by the NFI-RTLS AGV safety system to decide on the trajectory

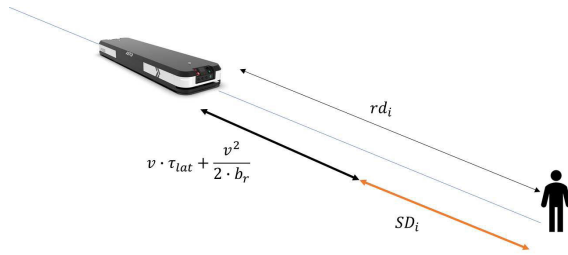


FIGURE 5. Relationship between the reaction distance and the safety distance.

of the AGV. If the tag is not located in the path of the AGV, even if it is within reaction distance r_d , the AGV does not need to change its trajectory. However, if the tag is located in the path, the AGV can decide whether to decelerate and stop, or change its trajectory. Thus, the AGV can decide on its trajectory autonomously, once the FCS provides it with the information about the origin station and the destination station.

Additionally, the information about the relative position of the tags from the AGV could be sent to the FCS. This way, the FCS could employ the information it receives from all the AGVs in the production plan to exploit low occupation zones and optimize the fleet movement. This will improve the intralogistics thereby increasing the productivity of the plant.

IV. RESULTS

The accuracy of the proposed NFI-RTLS AGV safety system will be analysed in this section. For this analysis, measurements were performed in two different scenarios. In the first scenario, some static measurements were made with a setup that emulated the size of the AGV. The objective of these measurements was to analyse the effect of applying the proposed ranging post-processing algorithm to the accuracy of the system. After that, the sensors were placed on a AGV of ASTI. Static and dynamic measurements were made to analyse the accuracy of the proposed system in a real environment.

A. METHODOLOGY

The accuracy of a positioning system is usually studied by observing the errors made in estimating the position. Sources of these errors include the imperfect performance from the transmitters and receivers, the characteristics of the channel and the inaccuracy of both the ranging and positioning estimators.

When we consider Cartesian coordinates in two dimensions, the distance error for the estimated position, ϵ_p is employed to analyze the accuracy of the positioning system:

$$\epsilon_p = \sqrt{(x - \hat{x})^2 + (y - \hat{y})^2}, \quad (6)$$

where (x, y) are the real Cartesian coordinates of the tag position and (\hat{x}, \hat{y}) represent the estimated coordinates of the tag position.

Positioning accuracy can also be measured when a polar coordinate system is employed. In fact, (5) clearly demon-

strated that the AGV reaction distance is related to the radius of the polar coordinate system, and thus it is more appropriate to analyze the accuracy of an AGV safety system in the polar coordinates. If we define (r, φ) as the real polar coordinates and $(\hat{r}, \hat{\varphi})$ as the estimated polar coordinates, we can define the error in the radius or radial error as:

$$\epsilon_r = |r - \hat{r}|, \quad (7)$$

and the error in the angle or angular error as:

$$\epsilon_\varphi = |\varphi - \hat{\varphi}|. \quad (8)$$

There are three main figures of merit that are traditionally used to determine the accuracy of a location system [48]: the mean of the error ϵ , the standard deviation (or the variance) and the Root Mean Square Error (RMSE). Thus, in this section these three figures of merit will be presented for the two measurement campaigns.

B. SYSTEM CONFIGURATION

Table 1 presents the main configuration parameters used in these measurements. The sensors and tags of the proposed safety system use the DW1000 chip of Decawave, which follows the IEEE 802.15.4 standard [49]. The UWB ranging distances between anchors and tag are obtained using the Two-Way Ranging (TWR) method described in [49]. These ranging distances are postprocessed using the algorithm explained in Section III-B, with the parameters shown in Table 1. Different communication protocols can be used in the proposed NFI-RTLS AGV safety system to handle multiple persons and multiple AGVs moving in the same space. In the results of this work, TWR-TDMA is being used, which is more than enough to monitor 16 people around an AGV. If we want to use the proposed system with a larger number of AGVs and tags, TDoA-TDMA is the most efficient solution according to [50]. The major drawback of a traditional FI-RTLS system using TDoA is that the clock of all anchors must be synchronized, which usually means that the anchors are connected by cables. This makes the installation of these anchors in the production plant even more cumbersome. However, in the case of the NFI-RTLS we are

TABLE 1. Configuration parameters of the UWB system.

Parameter	Value
Carrier frequency	3.9936 GHz
Bandwidth	499.2 MHz
Channel	2
Bitrate	6.8Mbps
PRF (pulse repetition frequency)	16 MHz
Preamble length	128 symbols
Preamble code	3
SFD (start of frame delimiter)	8 symbols
Latency	300 ms
Positioning rate	3.3 Hz
Postprocessing parameter α	0.9558
Postprocessing parameter β	0.2324

proposing, connecting the sensors in the AGV is simple and, thus, TDoA-TDMA can be used to handle scalability.

C. FIRST MEASUREMENT CAMPAIGN: STATIC MEASUREMENTS WITH AN EMULATED AGV

In this first scenario, some static measurements were taken with a setup that emulated the size of the AGV. The objective of taking these measurements was to analyze the effect of applying the proposed method for post-processing ranging data to the accuracy of the system.

1) MEASUREMENT SETUP WITH AN EMULATED AGV

The first set of experiments were carried out at Ceit’s facilities in Donostia/San Sebastián (Spain). A device that emulated the dimensions of the AGV designed by ASTI was employed in this first measurement campaign. Fig. 6 shows the laboratory and the area used for the tests. A Leica DISTO D510 laser meter with a range of up to 200 m and accuracy of ± 1 mm was used to measure the positions of the sensors placed on the “emulated AGV” and the tag. Fig. 6 also shows the coordinate system of the “emulated AGV”.



FIGURE 7. Placement of the NFI-RTLS AGV safety system in the first measurement campaign.

Static tests were carried out with the tag being placed at different test points (TP) to evaluate the accuracy of the proposed safety system. Fig. 6 shows all the positions where the tag was measured, where TP_i represents the i^{th} position of the tag. In all cases, the height of the tag was 0.88 m. The AGV was always in the same place, and the origin of the coordinate system was located in the middle of the AGV. For each test point, 950 positioning estimates were recorded.

2) RESULTS WITH AN EMULATED AGV

In this section, the error in the polar coordinates is analyzed, as it is more helpful to study the accuracy of the proposed NFI-RTLS AGV safety system. Table 2 shows the figures of merit for radial error ϵ_r for the complete static experiment. The first column represents the average radial error and the second and third column show its standard deviation and RMSE respectively. Additionally, the fourth and fifth column show the maximum radial error the system will present in 90% and 99% of the cases respectively. The last column presents the maximum radial error measured in the experiments. The first row of Table 2 shows the figures of merit for the experiment with raw ranging estimates, i.e.: when no post-processing method is applied to the ranging data; and the second row shows them when the proposed post-processing method was applied to the data. Analogously, Table 3 shows the statistics for the angular error in the polar coordinates. We can observe in both tables the benefits of applying the proposed post-processing method to the

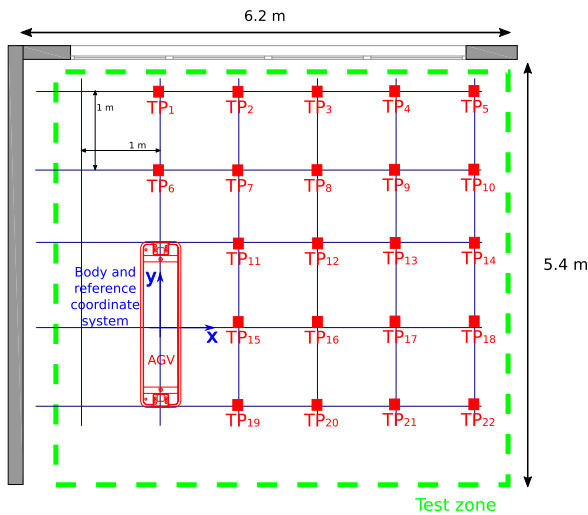


FIGURE 6. Layout of the laboratory for the first measurement campaign.

Fig. 7 shows a photograph of the laboratory set up. Sensors were installed on the “emulated AGV” and a tag was placed on a tripod, representing a worker or mobile asset.

TABLE 2. Radial error of the proposed NFI-RTLS AGV safety system in the first measurement campaign.

Ranging data	μ_{ϵ_r} (m)	σ_{ϵ_r} (m)	RMSE $_{\epsilon_r}$ (m)	$P = 90\%$ (m)	$P = 99\%$ (m)	$\max(\epsilon_r)$ (m)
No post-processing method	0.147	0.089	0.172	0.253	0.367	0.386
Proposed post-processing method	0.048	0.035	0.059	0.091	0.140	0.156

TABLE 3. Angular error of the proposed NFI-RTLS AGV safety system in the first measurement campaign.

Ranging data	μ_{ϵ_φ} (deg)	$\sigma_{\epsilon_\varphi}$ (deg)	RMSE $_{\epsilon_\varphi}$ (deg)	$P = 90\%$ (deg)	$P = 99\%$ (deg)	$\max(\epsilon_\varphi)$ (deg)
No post-processing method	3.216	1.673	3.626	5.547	6.995	8.426
Proposed post-processing method	1.910	1.211	2.262	3.507	4.888	6.219

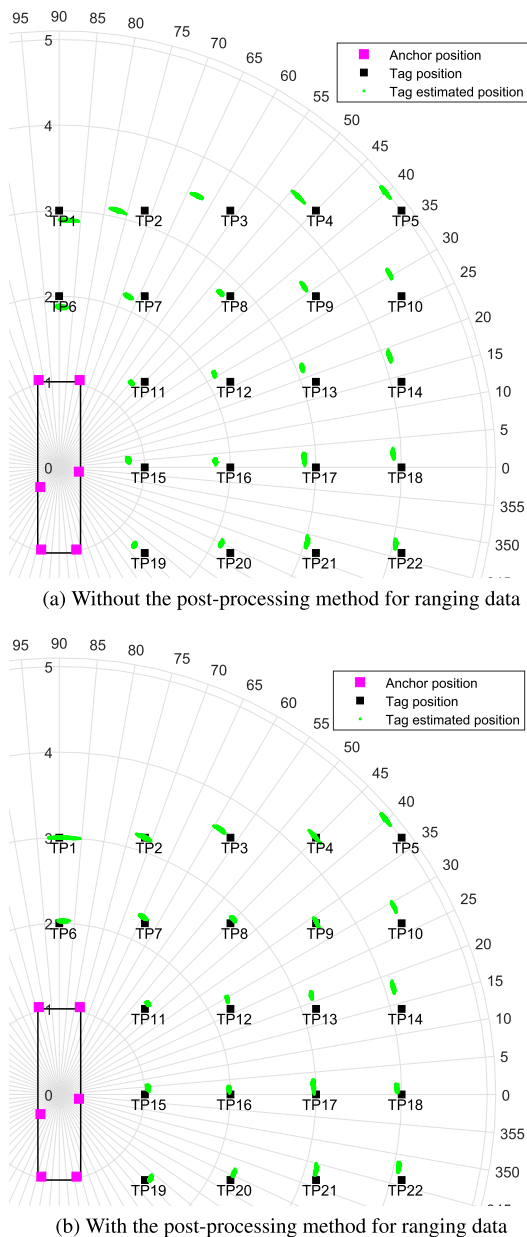


FIGURE 8. Positioning estimates in polar coordinates of the proposed NFI-RTLS AGV safety system for the first measurement campaign.

ranging estimates. The bias and standard deviation in both the radial and angular error are significantly reduced. Thus, using the proposed NFI-RTLS AGV safety system and this post-processing method for ranging data the safety system presents an RMSE of 0.059 m in the radial error and an RMSE of 2.262 degrees in the angular error.

When assessing a positioning system, it is also interesting to analyze the distribution of its error in the area of a room. Fig. 8 shows the points (black squares) in terms of polar coordinates in the first measurement campaign. The values in green are the positioning estimates from the proposed NFI-RTLS AGV safety system. Fig. 8a shows the positioning

estimates obtained when the ranging estimates are directly introduced in the positioning algorithm, and Fig. 8b presents the positioning values obtained after the ranging estimates were post-processed and before the positioning estimation was carried out. We can observe, once more, the benefits of applying a post-processing method to the ranging estimates. The positioning estimates in Fig. 8b are clearly more accurate than those in Fig. 8a. The proposed post-processing method for ranging data improves accuracy in the radius estimation in all measured points and reduces the error in the angle estimation in most of the points.

Fig. 9 depicts the distribution of the RMSE for the radial and angular error around the room. This figure shows the accuracy of the proposed NFI-RTLS AGV safety system at every room point, and the uniformity of the distribution of this error over the room. The real x and y coordinates of the measured positions correspond to the x -axis and y -axis respectively. The RMSE is gradated according to the color scale shown on the right side of the graphic, and depicted over the room area. Values in non-measured positions are calculated using the natural-neighbor interpolation in Matlab[®]. This interpolation is an improvement over linear interpolation, which works well with data that are not continuous over the room area [51], as is the case in this work. In the figures presented in this work, dark blue indicates a low RMSE value (higher accuracy) and dark yellow indicates a high RMSE (lower accuracy).

Fig. 9a and Fig. 9b show that the RMSE of the radial error is worse in estimating the position within close proximity of the AGV. Nevertheless, the RSME is clearly reduced when we apply the post-processing method to the ranging estimates. We also observe in Fig. 9c and Fig. 9d an improvement in the distribution of the RMSE of the angular error when the post-processing method is applied to the ranging data. In fact, the RMSE of both the radial and the angular error is smaller and more homogeneously distributed around the room. The results in this section shows that the NFI-RTLS AGV safety system clearly benefits from the post-processing method for ranging data that has been integrated in the NFI-RTLS AGV safety system.

3) COMPARISON WITH OTHER SAFETY SYSTEM

Table 4 compares the safety system from [24] and our proposed NFI-RTLS AGV safety system. This table presents the results of the best and worst test points of each system in terms of mean radial error, standard deviation, the radial error the system will present in 99% of the cases and maximum radial error.

Reference [24] proposes a collision avoidance system for AGVs based on UWB technology. This safety system uses only one anchor located on the AGV to calculate the relative distance between the tag and the AGV, but it is not able to provide the relative position between them. We can observe that the proposed NFI-RTLS AGV safety system performs significantly better than the one in [24]. The proposed NFI-RTLS AGV safety system has a maximum radial error of 0.156 m

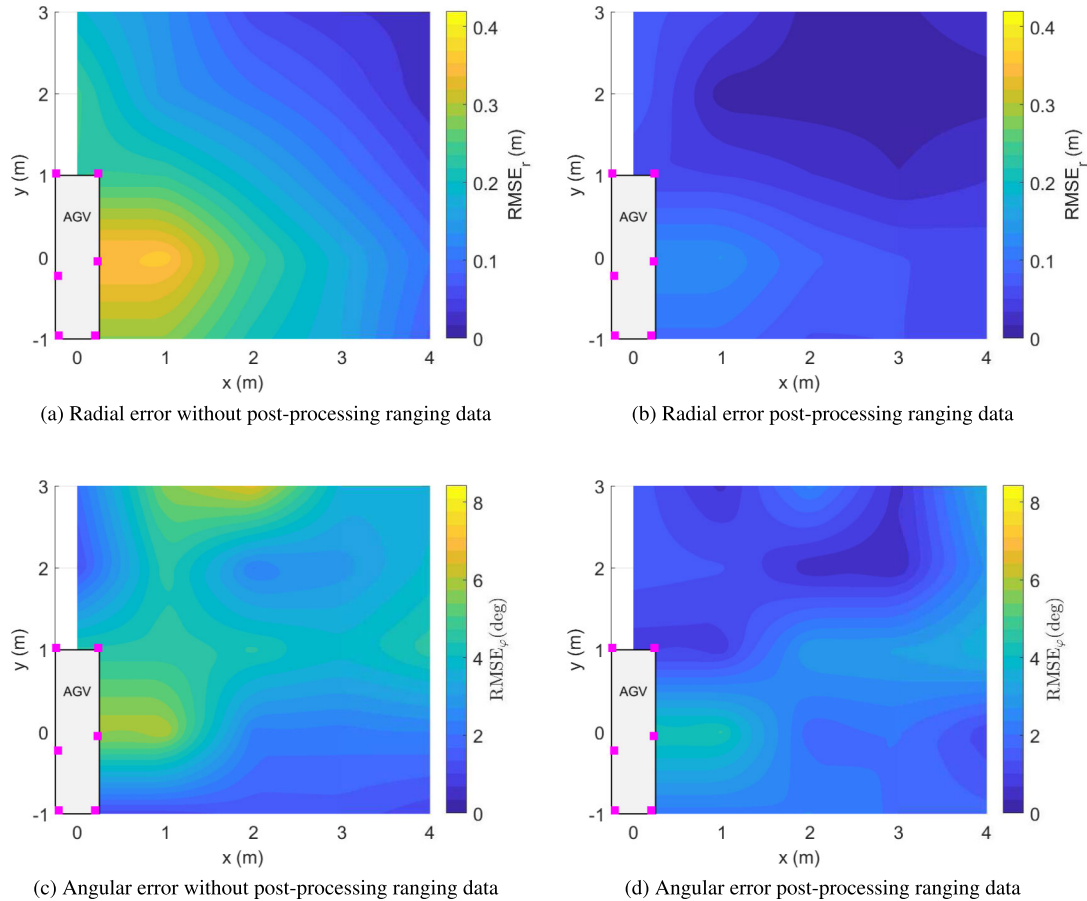


FIGURE 9. RMSE distribution around the room of the proposed NFI-RTLS AGV safety system in the first measurement campaign.

TABLE 4. Comparison between the proposed NFI-RTLS AGV safety system and another collision avoidance system in the literature.

Safety system	Test point	μ_{ϵ_r} (m)	σ_{ϵ_r} (m)	$P = 99\%$ (m)	$\max(\epsilon_r)$ (m)
[24]	best mean	0.031	0.029	n.a.	0.224
[24]	smallest max. error	0.087	0.013	n.a.	0.100
[24]	worst mean	12.260	1.421	n.a.	14.406
[24]	biggest max. error	7.986	9.682	n.a.	35.624
[24]	All	1.427	0.866	n.a.	35.624
NFI-RTLS AGV	TP8	0.006	0.004	0.018	0.023
NFI-RTLS AGV	TP15	0.135	0.007	0.151	0.156
NFI-RTLS AGV	All	0.048	0.035	0.140	0.156

whereas the maximum error in [24] is more than 100 times greater.

It should be mentioned that the test carried out in [24] is performed in a bigger area than ours, and that their environment is a real factory in contrast with our laboratory environment, which may be accountable for these large outliers. However, these outliers in [24] can make this collision avoidance system unstable or unsafe in certain situations and, thus, they should be detected and corrected. In contrast, the NFI-RTLS AGV safety system combined with the proposed post-processing method for ranging data is able to

eliminate big outliers and reduce the mean and maximum error to only a few centimeters, which will allow the AGV to safely navigate around people.

D. SECOND MEASUREMENT CAMPAIGN: DYNAMIC EXPERIMENTAL RESULTS WITH THE AGV

For the second measurement campaign, the sensors were placed on an AGV designed by ASTI. Dynamic measurements were taken to analyze the accuracy of the proposed system in a real environment.

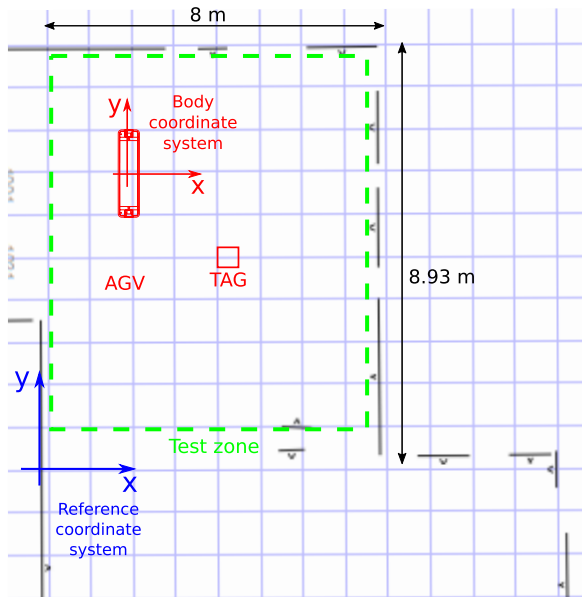


FIGURE 10. Layout of the ASTI Mobile Robotics laboratory used in the second measurement campaign.

1) MEASUREMENT SETUP WITH AGV

The experiments were carried out in the ASTI Mobile Robotics laboratory in Madrigalejo del Monte (Burgos, Spain) with a real AGV. Fig. 10 shows the laboratory and the area used for the tests. The laboratory was equipped with an Optitrack positioning system which allowed the AGV to be located within the laboratory with an accuracy of millimeters. In this work, the optical coordinate system is referred to as the “reference coordinate system”. Fig. 10 also shows an UWB tag and the AGV equipped with the UWB sensors of the proposed NFI-RTLS AGV safety system. The local coordinate system of the NFI-RTLS AGV safety system was aligned with the AGV’s body coordinate system and was located in the center of the AGV. Fig. 11 is a photograph showing the NFI-RTLS AGV safety system’s UWB sensors installed on the AGV and a UWB tag placed at a point in the laboratory.

The AGV used for the test was a BidiBot 2.0 designed by ASTI [52]. This AGV is an agile, flexible and intelligent system that can navigate using Quick Response (QR) codes, Simultaneous Localization and Mapping (SLAM) and magnetic lines. The AGV’s dimensions are 2104 x 500 x 230 mm (LxWxH) and it weighs 300 kg. At the time these measurements were taken, the AGV contained two safety lasers, a safety Programmable Logic Controller (PLC) and two emergency stop buttons, as well as different communication interfaces, Universal Serial Bus (USB) and Ethernet. The robot could be controlled manually or it could move automatically in every direction at a maximum speed of 2 m/s without load. Fig. 12 shows a photograph of this robot.

Dynamic tests were run at the ASTI facilities to evaluate the performance of the proposed NFI-RTLS AGV safety system. In these dynamic tests, the tag was positioned at one

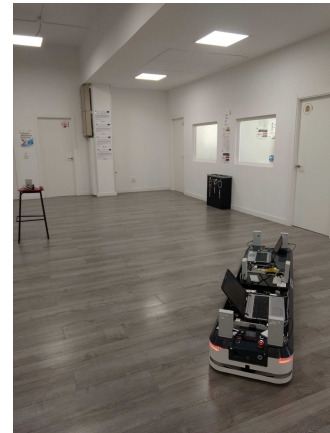


FIGURE 11. Taking measurements in the ASTI Mobile Robotics laboratory.



FIGURE 12. ASTI Mobile Robotics Bidibot 2.0.

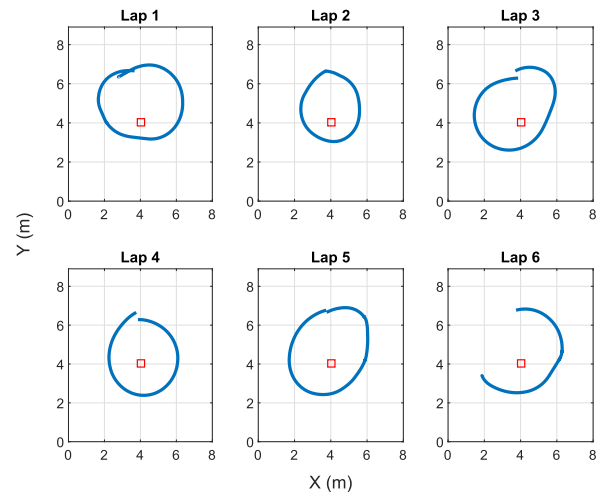


FIGURE 13. Dynamic laps in the reference coordinate system for the second measurement campaign.

point in the laboratory and the AGV moved around it in a circular movement. The position of the AGV (center of the AGV) and the position of the tag were obtained with the optical system and considered to be their real positions, i.e.: the optical system is used as a ground truth in this work, similarly to [15]. Furthermore, the positions calculated by the proposed NFI-RTLS AGV safety system were recorded and time-synchronized so that they could be compared with this ground truth. Fig. 13 shows the movement of the AGV recorded by the optical system in each of the laps taken (blue points), and the position of the stationary tag (red square).

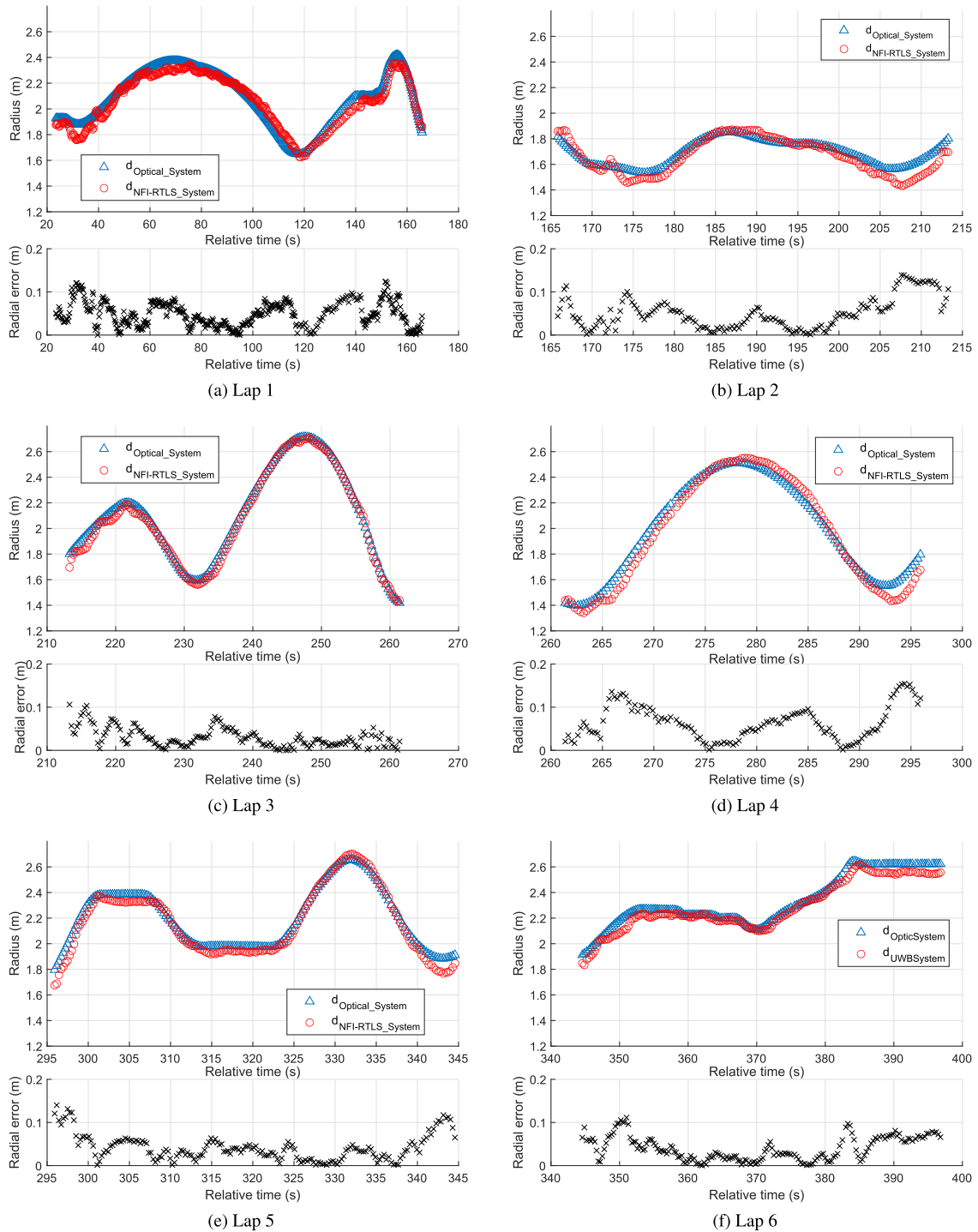


FIGURE 14. Dynamic test results for the proposed NFI-RTLS AGV safety system.

2) RESULTS

In this section, we present some results for the dynamic tests that were performed with the NFI-RTLS AGV safety system located in a moving AGV and when the tag remains static. Fig. 14 shows the results for the different laps taken and considering a polar coordinate system. For each lap, the top graphic compares the real radius measured with the optical

system with the radius estimated using the NFI-RTLS AGV system. The bottom graph shows the radial error. The evolution of these measurements is shown over time in Fig. 14. Taken together, they illustrate that this error is always below 16 cm and how the NFI-RTLS AGV system mirrors the movement of the AGV perfectly and accurately calculates the position of the tag relative to the AGV.

Table 5 presents the main statistics for each lap, and the values of the figure of merit when all laps are considered. Each lap was performed with different speeds or movements, and these factors did not lead to significant degradation in accuracy. The NFI-RTLS AGV safety system presents a mean radial error of 4.5 cm and a RMSE of 5.5 cm. These accuracy results are similar to those obtained by the ATLAS system when it was installed in an ASTI's AGV [12]. However, the ATLAS system requires placing anchors on the infrastructure in order to provide a position estimation for the tag placed on the AGV. The proposed NFI-RTLS AGV safety system provides better accuracy without requiring hardware be placed on the plant's infrastructure. Moreover, our proposal is a more flexible solution and requires low deployment costs, as no fixed infrastructure is needed.

TABLE 5. Radial error of the proposed NFI-RTLS AGV safety system in each lap of the dynamic test.

	μ_{ϵ_r} (m)	σ_{ϵ_r} (m)	$RMSE_{\epsilon_r}$ (m)	$P = 90\%$ (m)	$P = 99\%$ (m)	$\max(\epsilon_r)$ (m)
Lap 1	0.048	0.028	0.056	0.086	0.120	0.124
Lap 2	0.051	0.037	0.062	0.118	0.139	0.139
Lap 3	0.030	0.023	0.037	0.063	0.103	0.106
Lap 4	0.064	0.039	0.075	0.125	0.153	0.154
Lap 5	0.041	0.030	0.051	0.085	0.131	0.140
Lap 6	0.039	0.027	0.048	0.075	0.105	0.111
All	0.045	0.031	0.055	0.086	0.131	0.154

TABLE 6. Statistics for the proposed NFI-RTLS AGV safety system.

	True Positive	False Positive	True Negative	False Negative
All laps	41.47%	2.62%	55.03%	0.88%

The proposed NFI-RTLS AGV safety system can be used to decide when the radius of the polar coordinate system for the tag is below the reaction distance r_{d_i} defined in (5) and react by reducing the AGVs maximum cruise velocity as defined in (3). In Table 6, we can observe the statistics associated when a reaction distance r_{d_i} of 2 m is considered in the dynamic tests performed in ASTI's AGV. In this table, a reaction is considered positive whenever the AGV is below this reaction distance. The NFI-RTLS AGV safety system produces a true estimate for 96.5% of the cases; in only 0.88% of the cases the system estimates that the tag is further from this limit when it is actually below the reaction distance. In fact, the maximum error in the radius estimates in the proposed NFI-RTLS AGV safety system is only 8 cm when there is a false negative and 12 cm when there is a false positive.

V. CONCLUSION

Although there are works in the literature that have proposed RTLS-based navigation systems that locate obstacles in an

AGV's path and complement the information from other sensors in the AGV, those works require hardware (anchors) be installed on plant's infrastructure. Moreover, those systems need to be deployed carefully, as anchor placement tends to affect the accuracy of the RTLS system. In highly-flexible production environments, this can be a big drawback in deploying of the FI-RTLS AGV safety systems. Furthermore, this kind of safety system often requires an ultra-low latency communication link between the fleet control system and the AGVs in a fleet, if those commands are going to be used to stop the AGV or change its trajectory. But achieving this ultra-low latency communication link is not always possible in a real industrial environment.

This work presents a different approach that exploits the high positioning accuracy of UWB technology, without the need to install any hardware on the plant's infrastructure. This solution saves money and simplifies the deployment of an AGV fleet in a production plant. Furthermore, it enables AGVs to be used safely in the highly-flexible Industry 4.0 production scenario. The proposed NFI-RTLS AGV safety system consists of a set of UWB sensors that are placed on the mobile robot that will locate the tags worn by people or mobile assets. This safety system provides the AGV with individual identification and 2-D positioning for the tags around it. Thus, the AGV can react rapidly when needed. Moreover, this reaction can differ depending on the location as well as the identity of the tag.

The proposed NFI-RTLS system employs a method to post-process ranging data that only requires a simple calibration to be performed during the production phase of the AGV. The experimental results in this paper have shown that this method reduces both the bias and the variance of error in the radius and angle estimates. Moreover, results show that the estimation errors in both the angle and the radius are homogeneously distributed around the room. For an AGV safety system, a high degree of accuracy is critical when the tag is close to the AGV, as this is where collisions can occur. Using the proposed post-processing method, the positioning accuracy of the proposed NFI-RTLS AGV safety system is improved especially in the proximity of the AGV.

A collision avoidance system that does not require installing hardware on plant infrastructure was recently proposed in the literature. However, that system only was able to estimate the radius, and thus it was not able to determine the exact location of the tag. In comparing that work with the NFI-RTLS AGV safety system proposed here, our system presents much better accuracy in the radius estimation. Furthermore, our system is able to estimate the angle with a small error, which allows the AGV to locate the positions of the tags around it with a high degree of accuracy.

Finally, the proposed NFI-RTLS AGV safety system was mounted on an AGV designed by the company ASTI Mobile Robotics. Dynamic measurements were performed, showing that the proposed safety system tracks the relative movement between the AGV and tag with no significant degradation in accuracy. In fact, the resulting accuracy is similar to other

FI-RTLS based safety systems in the literature that require hardware to be installed on plant infrastructure. The experimental results show that good accuracy can be obtained without requiring any hardware being added to the plant infrastructure.

ACKNOWLEDGMENT

The authors would like to thank their teams at CEIT and ASTI.

REFERENCES

- [1] S. Weyer, M. Schmitt, M. Ohmer, and D. Gorecky, "Towards industry 4.0 standardization as the crucial challenge for highly modular, multi-vendor production systems," *IFAC-PapersOnLine*, vol. 48, no. 3, pp. 579–584, 2015.
- [2] G. Fragapane, D. Ivanov, M. Peron, F. Sgarbossa, and J. O. Strandhagen, "Increasing flexibility and productivity in industry 4.0 production networks with autonomous mobile robots and smart intralogistics," *Ann. Oper. Res.*, pp. 1572–9338, Feb. 2020, doi: 10.1007/s10479-020-03526-7.
- [3] *Industrial Trucks—Safety Requirements and Verification—Part 4: Driverless Industrial Trucks and Their Systems*, Standard ISO 3691-4:2020(en), 2020. Accessed: May 5, 2020. [Online]. Available: <https://www.iso.org/obp/ui/#iso:std:iso:3691-4:ed-1:v1:en>
- [4] E. Shi, Z. Wang, X. Huang, and Y. Huang, "Study on AGV posture estimating based on distributed Kalman fusion for multi-sensor," in *Proc. IEEE Int. Conf. Robot. Biomimetics (ROBIO)*, Dec. 2009, pp. 1219–1223.
- [5] X. Zhou, T. Chen, and Y. Zhang, "Research on intelligent AGV control system," in *Proc. Chin. Autom. Congr. (CAC)*, Nov. 2018, pp. 58–61.
- [6] D. Shi, H. Mi, E. G. Collins, and J. Wu, "An indoor low-cost and high-accuracy localization approach for AGVs," *IEEE Access*, vol. 8, pp. 50085–50090, 2020.
- [7] J. Jiang, Y. Guo, and W. Liao, "Research on AGV guided by real-time locating system (RTLS) for material distribution," *Int. J. Control Autom.*, vol. 8, no. 7, pp. 213–226, Jul. 2015.
- [8] A. Alarifi, A. Al-Salman, M. Alsaleh, A. Alnafessah, S. Al-Hadhrami, M. Al-Ammar, and H. Al-Khalifa, "Ultra wideband indoor positioning technologies: Analysis and recent advances," *Sensors*, vol. 16, no. 5, p. 707, May 2016.
- [9] A. R. J. Ruiz and F. S. Granja, "Comparing ubisense, BeSpoon, and DecaWave UWB location systems: Indoor performance analysis," *IEEE Trans. Instrum. Meas.*, vol. 66, no. 8, pp. 2106–2117, Aug. 2017.
- [10] C. Kirsch and C. Röhrig, "Global localization and position tracking of an automated guided vehicle," *IFAC Proc. Volumes*, vol. 44, no. 1, pp. 14036–14041, 2011.
- [11] C. Kirsch, F. Künemund, D. Heß, and C. Röhrig, "Comparison of localization algorithms for AGVs in industrial environments," in *Proc. 7th German Conf. Robot. (ROBOTIK)*, Jan. 2012, pp. 183–188.
- [12] M. C. Pérez-Rubio, C. Losada-Gutiérrez, F. Espinosa, J. Macias-Guarasa, J. Tiemann, F. Eckeremann, C. Wietfeld, M. Katkov, S. Huba, J. Urefia, J. M. Villadangos, D. Gualda, E. Díaz, R. Nieto, E. Santiso, P. del Portillo, and M. Martínez, "A realistic evaluation of indoor robot position tracking systems: The IPIN 2016 competition experience," *Measurement*, vol. 135, pp. 151–162, Mar. 2019.
- [13] E. R. S. Santos, H. Azpurua, P. A. F. Rezeck, M. F. S. Corrêa, M. A. M. Vieira, G. M. Freitas, and D. G. Macharet, "Localization using ultra wideband and IEEE 802.15.4 radios with nonlinear Bayesian filters: A comparative study," *J. Intell. Robotic Syst.*, vol. 99, nos. 3–4, pp. 571–587, Sep. 2020.
- [14] X. Zhu, J. Yi, J. Cheng, and L. He, "Adapted error map based mobile robot UWB indoor positioning," *IEEE Trans. Instrum. Meas.*, vol. 69, no. 9, pp. 6336–6350, Sep. 2020.
- [15] M. Strohmeier, T. Walter, J. Rothe, and S. Montenegro, "Ultra-wideband based pose estimation for small unmanned aerial vehicles," *IEEE Access*, vol. 6, pp. 57526–57535, 2018.
- [16] C. Luo, W. Li, X. Fan, H. Yang, J. Ni, X. Zhang, G. Xin, and P. Shi, "Positioning technology of mobile vehicle using self-repairing heterogeneous sensor networks," *J. Netw. Comput. Appl.*, vol. 93, pp. 110–122, Sep. 2017.
- [17] P. Vasilyev, S. Pearson, M. El-Gohary, M. Aboy, and J. McNames, "Inertial and time-of-arrival ranging sensor fusion," *Gait Posture*, vol. 54, pp. 1–7, May 2017.
- [18] G. Ding, H. Lu, J. Bai, and X. Qin, "Development of a high precision UWB/vision-based AGV and control system," in *Proc. 5th Int. Conf. Control Robot. Eng. (ICCRE)*, Apr. 2020, pp. 99–103.
- [19] A. Benini, A. Mancini, and S. Longhi, "An IMU/UWB/vision-based extended Kalman filter for mini-UAV localization in indoor environment using 802.15.4a wireless sensor network," *J. Intell. Robotic Syst.*, vol. 70, nos. 1–4, pp. 461–476, Apr. 2013.
- [20] X. An, S. Zhao, X. Cui, Q. Shi, and M. Lu, "Distributed multi-antenna positioning for automatic-guided vehicle," *Sensors*, vol. 20, no. 4, p. 1155, Feb. 2020.
- [21] B. Zhu, X. Tao, J. Zhao, M. Ke, H. Wang, and W. Deng, "An integrated GNSS/UWB/DR/VMM positioning strategy for intelligent vehicles," *IEEE Trans. Veh. Technol.*, vol. 69, no. 10, pp. 10842–10853, Oct. 2020.
- [22] M. Wang, X. Chen, B. Jin, P. Lv, W. Wang, and Y. Shen, "A novel V2V cooperative collision warning system using UWB/DR for intelligent vehicles," *Sensors*, vol. 21, no. 10, p. 3485, May 2021.
- [23] R. Rey, J. A. Cobano, M. Corzetto, L. Merino, P. Alvito, and F. Caballero, "A novel robot co-worker system for paint factories without the need of existing robotic infrastructure," *Robot. Comput.-Integr. Manuf.*, vol. 70, Aug. 2021, Art. no. 102122.
- [24] S. Monica and G. Ferrari, "Low-complexity UWB-based collision avoidance system for automated guided vehicles," *ICT Exp.*, vol. 2, no. 2, pp. 53–56, Jun. 2016.
- [25] L. Zamora-Cadenas, N. Arrue, A. Jimenez-Iratorza, and I. Velez, "Improving the performance of an FMCW indoor localization system by optimizing the ranging estimator," in *Proc. 6th Int. Conf. Wireless Mobile Commun.*, Sep. 2010, pp. 226–231.
- [26] H. Perakis and V. Gikas, "Evaluation of range error calibration models for indoor UWB positioning applications," in *Proc. Int. Conf. Indoor Positioning Indoor Navigat. (IPIN)*, Sep. 2018, pp. 206–212.
- [27] A. D. Preter, G. Goysens, J. Anthonis, J. Swevers, and G. Pipeleers, "Range bias modeling and autocalibration of an UWB positioning system," in *Proc. Int. Conf. Indoor Positioning Indoor Navigat. (IPIN)*, Sep. 2019, pp. 1–8.
- [28] L. Wiebking, M. Vossiek, L. Reindl, M. Christmann, and D. Mastela, "Precision local positioning radar with implemented extended Kalman filter," in *Proc. Eur. Conf. Wireless Technol.*, 2003, pp. 459–462.
- [29] Y. Chu and A. Ganz, "A UWB-based 3D location system for indoor environments," in *Proc. 2nd Int. Conf. Broadband Netw.*, vol. 2, 2005, pp. 1147–1155.
- [30] D. Mastela, L. Reindl, L. Wiebking, M. Kawalkiewicz, and T. Zander, "Angle tracking using FMCW radar based localization system," in *Proc. Int. Radar Symp.*, May 2006, pp. 1–4.
- [31] P. Tragas, A. Kalis, C. Papadias, F. Ellinger, R. Eickhoff, T. Ussmuller, R. Mosshammer, M. Huemer, A. Dabek, D. Doumenis, and A. Kounoudes, "RESOLUTION: Reconfigurable systems for mobile local communication and positioning," in *Proc. 16th IST Mobile Wireless Commun. Summit*, Jul. 2007, pp. 216–220.
- [32] F. Ellinger, R. Eickhoff, A. Zirolli, J. Hütner, R. Gierlich, J. Carls, and G. Böck, "European project RESOLUTION-local positioning systems based on novel FMCW radar," in *IEEE MTT-S Int. Microw. Symp. Dig.*, Oct. 2007, pp. 499–502.
- [33] C. Röhrig and S. Spieker, "Tracking of transport vehicles for warehouse management using a wireless sensor network," in *Proc. IEEE/RSJ Int. Conf. Intell. Robots Syst.*, Sep. 2008, pp. 3260–3265.
- [34] L. Liu, E. Manli, Z. Wang, and M. Zhou, "A 3D self-positioning method for wireless sensor nodes based on linear FMCW and TFDA," in *Proc. IEEE Int. Conf. Syst., Man Cybern.*, Oct. 2009, pp. 2990–2995.
- [35] H. Cho, C.-W. Lee, S.-J. Ban, and S.-W. Kim, "An enhanced positioning scheme for chirp spread spectrum ranging," *Expert Syst. Appl.*, vol. 37, no. 8, pp. 5278–5735, Aug. 2010.
- [36] L. Liu and E. Manli, "Improve the positioning accuracy for wireless sensor nodes based on TFDA and TFOA using data fusion," in *Proc. Int. Conf. Netw., Sens. Control (ICNSC)*, Apr. 2010, pp. 32–37.
- [37] Y. Zhou, C. L. Law, and F. Chin, "Construction of local anchor map for indoor position measurement system," *IEEE Trans. Instrum. Meas.*, vol. 59, no. 7, pp. 1986–1988, Jul. 2010.

- [38] D. Kang, Y. Namgoong, S. Yang, S. Choi, and Y. Shin, "A simple asynchronous UWB position location algorithm based on single round-trip transmission," in *Proc. 8th Int. Conf. Adv. Commun. Technol.*, vol. 3, Feb. 2006, pp. 1458–1461.
- [39] Y. Nam, H. Lee, J. Kim, and K. Park, "Two-way ranging algorithms using estimated frequency offsets in WPAN and WBAN," in *Proc. 3rd Int. Conf. Conver. Hybrid Inf. Technol.*, vol. 1, Nov. 2008, pp. 842–847.
- [40] N. Arrue, M. Losada, L. Zamora-Cadenas, A. Jimenez-Irastorza, and I. Velez, "Design of an IR-UWB indoor localization system based on a novel RTT ranging estimator," in *Proc. 1st Int. Conf. Sensor Device Technol. Appl.*, Jul. 2010, pp. 52–57.
- [41] A. A. D'Amico, L. Taponecco, and U. Mengali, "Ultra-wideband TOA estimation in the presence of clock frequency offset," *IEEE Trans. Wireless Commun.*, vol. 12, no. 4, pp. 1606–1616, Apr. 2013.
- [42] S. Sharma, V. Bhatia, and A. Gupta, "Joint symbol and ToA estimation for iterative transmitted reference pulse cluster UWB system," *IEEE Syst. J.*, vol. 13, no. 3, pp. 2629–2640, Sep. 2019.
- [43] J. Joung, S. Jung, S. Chung, and E. Jeong, "CNN-based Tx–Rx distance estimation for UWB system localisation," *Electron. Lett.*, vol. 55, no. 17, pp. 938–940, Aug. 2019.
- [44] E. Karapistoli, F. Pavlidou, I. Gragopoulos, and I. Tsetsinas, "An overview of the IEEE 802.15.4a Standard," *IEEE Commun. Mag.*, vol. 48, no. 1, pp. 47–53, Jan. 2010.
- [45] K. Muthukrishnan and M. Hazas, "Position estimation from UWB pseudorange and angle-of-arrival: A comparison of non-linear regression and Kalman filtering," in *Proc. 4th Int. Symp. Location Context Awareness (LoCA)*. Berlin, Germany: Springer-Verlag, 2009, pp. 222–239.
- [46] T. Otim, A. Bahillo, L. E. Díez, P. Lopez-Iturri, and F. Falcone, "Towards sub-meter level UWB indoor localization using body wearable sensors," *IEEE Access*, vol. 8, pp. 178886–178899, 2020.
- [47] S. M. Kay, *Fundamentals of Statistical Signal Processing: Estimation Theory*, 1st ed. Upper Saddle River, NJ, USA: Prentice-Hall, 1993.
- [48] R. Y. Rubinstein, *Simulation and the Monte Carlo Method*, 1st ed. Hoboken, NJ, USA: Wiley, 1981.
- [49] Decawave. (Accessed: May 30, 2021). *DW1000 User Manual Version 2.18*. Accessed: 2017. [Online]. Available: <https://www.decawave.com/dw1000/usermanual/>
- [50] M. Ridolfi, S. Van De Velde, H. Steendam, and E. De Poorter, "Analysis of the scalability of UWB indoor localization solutions for high user densities," *Sensors*, vol. 18, no. 6, p. 1875, Jun. 2018. [Online]. Available: <https://www.mdpi.com/1424-8220/18/6/1875>
- [51] The MathWorks, Inc. (Accessed: May 30, 2021). *Interpolating Scattered Data With MATLAB Software*. Accessed: 2021. [Online]. Available: <http://www.mathworks.es/es/help/matlab/math/interpolating-scattered-data.html>
- [52] Asti Mobile Robotics. *Platform AGVs*. Accessed: May 30, 2021. [Online]. Available: <https://www.astimobilerobotics.com/platform-agvs>



LETICIA ZAMORA-CADENAS was born in León, Spain. She received the B.Sc. and M.Sc. degrees in telecommunications engineering from the University of Valladolid, Spain, in 2005 and 2008, respectively, and the Ph.D. degree in electrical and electronics engineering from the Universidad de Navarra, in 2014.

She has been a Research Staff Member of CEIT, San Sebastian, Spain, since 2008, and a Lecturer with the University of Navarra, since 2014. Her research interests include localization systems, positioning algorithms and bayesian filtering, and data fusion and signal processing for telecommunication systems.



IGONE VELEZ was born in Mondragón, Spain, in 1977. She received the M.Sc. degree in electrical, electronic and control engineering and the Ph.D. degree from the University of Navarra, Spain, in 2000 and 2005, respectively.

She has been a Research Staff Member of CEIT, San Sebastian, Spain, since 2000, and an Associate Professor with the University of Navarra, since 2005. She is currently the Director of the ICT Division, CEIT. She has been involved in international and national projects related to UWB, RFID, and 5G technologies. Her current research interests include signal processing and hardware development for telecommunication systems and positioning systems.



J. ENRIQUE SIERRA-GARCIA was born in Burgos, in 1983. He received the degrees in electronics engineering, telecommunications engineering, and control engineering, the Ph.D. degree in computer science, and the M.B.A. degree. He has been the principal researcher in many research projects related to mobile robotics and AGVs. In addition, his professional experience includes almost 15 years working as a researcher and a software and hardware engineer in several companies. He is currently a Senior Lecturer with the Department of Electromechanical Engineering, University of Burgos. He is also the Creator of ASTI-UBU Joint Research Unit on autonomous vehicles, mobile robotics and AGVs. His research interests include robotics, modelling, intelligent control, and soft computing techniques.

...